

# Novel Approach to Measuring the Penetration Depth Anisotropy in MgB<sub>2</sub> Using Small-Angle Neutron Scattering

D. Pal,<sup>1</sup> L. DeBeer-Schmitt,<sup>1</sup> T. Bera,<sup>1</sup> R. Cubitt,<sup>2</sup> C. D. Dewhurst,<sup>2</sup> J. Jun,<sup>3</sup> N. D. Zhigadlo,<sup>3</sup> J. Karpinski,<sup>3</sup> V. G. Kogan,<sup>4</sup> and M. R. Eskildsen<sup>1,\*</sup>

<sup>1</sup>*Department of Physics, University of Notre Dame, Notre Dame, IN 46556*

<sup>2</sup>*Institut Laue-Langevin, 6 Rue Jules Horowitz, F-38042 Grenoble, France*

<sup>3</sup>*Laboratory for Solid State Physics, ETH, CH-8093 Zürich, Switzerland*

<sup>4</sup>*Ames Laboratory and Department of Physics and Astronomy, Iowa State University, Ames, Iowa 50011*

(Dated: March 22, 2019)

Using small-angle neutron scattering we have measured the misalignment between an applied field of 4 kOe and the flux-line lattice in MgB<sub>2</sub>, as the field is rotated away from the *c* axis by an angle  $\theta$ . The measurements, performed at 4.9 K, showed the vortices canting towards the *c* axis for all field orientations. Using a two-band/two-gap model to calculate the magnetization we are able to fit our results yielding a penetration depth anisotropy,  $\gamma_\lambda = 1.1 \pm 0.1$ .

PACS numbers: 74.25.Qt, 74.70.Ad, 61.12.Ex, 74.20.-z

The two-band/two-gap nature of superconductivity in Magnesium diboride (MgB<sub>2</sub>) is well established.<sup>1</sup> In this material supercarriers reside on two distinctively different parts of the Fermi surface, with the larger energy gap ( $\Delta_\sigma \approx 7$  meV) originating from  $\sigma$  bonding of *p*<sub>xy</sub> boron orbitals, and the smaller gap ( $\Delta_\pi = 2.2$  meV) arising from  $\pi$  bonding of the *p*<sub>z</sub> orbitals.<sup>2,3,4</sup> Furthermore the  $\pi$  band is isotropic, while the  $\sigma$  band is nearly two-dimensional.

The anisotropy of a type-II superconductor is described either by  $\gamma_\lambda = \lambda_c/\lambda_{ab}$ , where  $\lambda$  is the magnetic penetration depth, or by  $\gamma_H = H_{c2,ab}/H_{c2,c} = \xi_{ab}/\xi_c$ , with  $\xi$  being the coherence length. Traditionally these two anisotropies have been considered to be identical, but in materials with anisotropic gaps this is generally not the case.<sup>5,6,7</sup> Magnesium diboride represents an extreme case where  $\gamma_H \neq \gamma_\lambda$ . Theoretical work for this material indicates  $\gamma_\lambda(0) \approx 1.1$  and  $\gamma_H(0) \approx 6$  at low temperatures, merging at  $\gamma_\lambda(T_c) = \gamma_H(T_c) \approx 2.6$  at the critical temperature  $T_c$ .<sup>5,7,8</sup>

While there is experimental consensus on the temperature dependence of  $\gamma_H$ ,<sup>9,10,11,12,13,14,15</sup> it has recently been suggested that superconductivity in MgB<sub>2</sub> can be described by a single anisotropy factor,  $\gamma(H) = \gamma_\lambda(H) = \gamma_\xi(H)$ , changing from  $\gamma(H = 0) \sim 1$  to  $\gamma(H = H_{c2}) \sim 6$ .<sup>14,16</sup> However, measurements of  $\gamma_\lambda(H)$  are still contradictory, with flux-line lattice imaging and torque magnetometry measurements yielding results ranging from an arguably field-independent value of  $\gamma_\lambda \approx 1.2$ ,<sup>17,18,19</sup> to a strongly field-dependent  $\gamma_\lambda$  increasing with field and attaining a value of  $\sim 3.5$  at a modest field of 5 kOe.<sup>16,20</sup> Measurements of the electronic specific heat in MgB<sub>2</sub>, which mainly reflects  $\gamma_\xi$  yields an anisotropy which increases with the applied field.<sup>21</sup>

In this paper we will demonstrate a novel use of small-angle neutron scattering (SANS) to determine the penetration depth anisotropy in MgB<sub>2</sub>, by measuring the misalignment between the applied field,  $\mathcal{H}$ , and the direction of the vortices in the flux-line lattice (FLL) as the

field is rotated between the *c* axis and the basal plane. Using a two-band/two-gap model we can fit the angular dependence of the misalignment. At 4.9 K and 4 kOe we find  $\gamma_\lambda = 1.1 \pm 0.2$ , smaller than SANS measurements of the FLL anisotropy in single crystals<sup>20</sup> and torque magnetometry<sup>16</sup>, but in good agreement with SANS results on powders<sup>17</sup> and scanning tunneling spectroscopy results.<sup>18</sup> The misalignment corresponds to vortices canting towards the crystalline *c* axis.

The experiments were performed at the NG3 SANS instrument at the NIST Center for Neutron Research. The sample was a  $\sim 200$   $\mu\text{g}$  platelike single crystal with the *c* axis parallel to the thin direction, grown using isotopically enriched <sup>11</sup>B to reduce neutron absorption<sup>22</sup>. The <sup>11</sup>B concentration in the sample is estimated to be  $\sim 95\%$ , with  $\sim 5\%$  <sup>10</sup>B due to the use of a natural boron BN crucible (20% <sup>10</sup>B, 80% <sup>11</sup>B) in the crystal growth. Incident neutrons with a wavelength  $\lambda_n = 1$  nm and a wavelength spread  $\Delta\lambda_n/\lambda_n = 14\%$  were used, and the FLL diffraction pattern was collected by a 650 mm  $\times$  650 mm position sensitive detector with 5 mm resolution. Both the collimation and sample-to-detector distances were 8 m. All measurements were performed in a magnetic field of 4 kOe applied at different angles,  $\theta = 0^\circ - 80^\circ$ , with respect to the crystalline *c* axis. For all angles the field was rotated around the vertical crystalline [110] axis (see Fig. 1(a)), and the measurements were obtained following a field cooling procedure to a temperature of 4.9 K.

Fig. 1 shows FLL diffraction patterns obtained for three different orientations of the applied field. Each image is a sum of the scattering from the FLL as the cryomagnet is rotated around the vertical axis in order to satisfy the Bragg condition for the different reflections. In Fig. 1(a) the field is applied parallel to both the sample *c* axis ( $\theta = 0^\circ$ ) as well as the direction of the neutron beam. Consistent with our earlier reports a hexagonal FLL is observed, with the lattice plane normals (Bragg peaks) along the *a* axis.<sup>20</sup> Applying the field at an

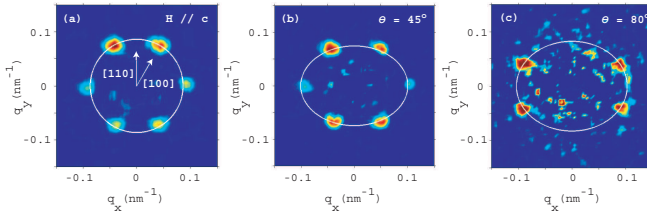


FIG. 1: FLL diffraction patterns for  $\text{MgB}_2$  obtained at 4 kOe and 4.9 K, and with the applied field at angles  $\theta = 0^\circ$  (a),  $45^\circ$  (b), and  $80^\circ$  (c) with respect to the  $c$  axis. The orientation of the sample crystallographic axes are shown in panel (a). The reflection on the vertical axis in panel (c) are absent since they do not satisfy the Bragg condition. The data are smoothed by a  $5 \times 5$  box average.

gle with respect to the  $c$  axis leads to a distortion of the hexagonal FLL as shown in Fig. 1(b), and eventually a reorientation shown in Fig. 1(c). In contrast to  $\mathcal{H} \parallel c$  where the reorientation progresses continuously above an onset field  $H^* \sim 5$  kOe,<sup>20</sup> the transition in rotated fields is first order and occurs at  $\theta \sim 70^\circ$  with an applied field of 4 kOe. The FLL reorientation is attributed to the multi-gap nature of the superconductivity in this material.<sup>20,23</sup> Previously the FLL anisotropy has been used as a measure of  $\gamma_\lambda$ .<sup>18,20</sup> However, recent measurements have indicated that this anisotropy may be influenced by vortex core effects,<sup>24</sup> similar to what is observed in members of the borocarbide superconductors.<sup>25</sup>

The exact orientation of the applied magnetic field is obtained from the FLL rocking curve with  $\mathcal{H} \parallel c$ . In this case the vortices are parallel to the applied field. In Fig. 2(a) the intensities of the Bragg peaks lying on the horizontal axis are plotted as a function of the cryomagnet rotation angle,  $\alpha$ . The calibrated zero ( $\alpha = 0$ ) is determined from the position of the midpoint between the two peaks, obtained by Gaussian fits to the rocking curves. As the field is rotated away from the  $c$  axis the vortices in the FLL cant away from the direction of the applied field as shown in Figs. 2(b) and 2(c). The rocking curve midpoint now directly reflects the misalignment of the FLL,  $\delta\theta$ , with respect to the direction of the applied field. Note that above the FLL reorientation transition four Bragg peaks shown in Fig. 1(c) are centered around the horizontal axis and used to determine  $\delta\theta$ . The misalignment corresponds to the vortices being rotated towards the crystalline  $c$  axis. Only a slight increase in the average rocking curve width from  $0.45^\circ \pm 0.05^\circ$  FWHM ( $\theta = 0^\circ$ ) to  $0.55^\circ \pm 0.05^\circ$  FWHM ( $\theta = 80^\circ$ ) is observed as the field is rotated away from the  $c$  axis, indicating that no significant disordering of the FLL takes place. The experimental resolution is estimated to be  $\sim 0.25^\circ$  FWHM. The absolute scattered intensity from the FLL decreases due to the increased absorption, as the effective sample thickness becomes larger.

The results of the SANS measurements are summarized in Fig. 3. This shows a symmetrical  $\delta\theta$  vs.  $\theta$  dependence, with a maximum  $\delta\theta \simeq 1^\circ$  close to  $\theta = 45^\circ$ ,

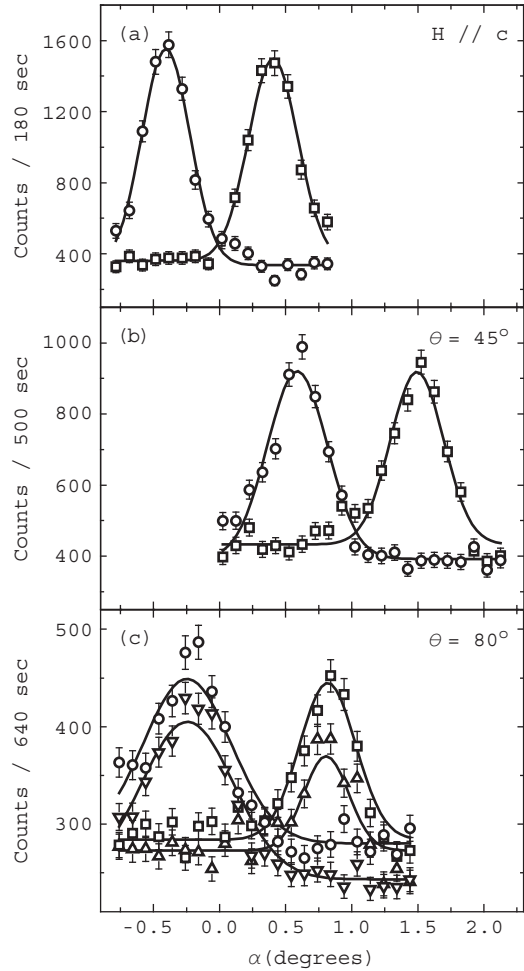


FIG. 2: FLL rocking curves for  $\text{MgB}_2$  with the applied field at  $\theta = 0^\circ$  (a),  $45^\circ$  (b), and  $80^\circ$  (c) with respect to the  $c$  axis. The intensities at each angular setting,  $\alpha$ , is obtained by summing the detector counts at position of the Bragg reflections. The curves are Gaussian fits to the data. No background subtraction is performed.

and decreasing towards zero for  $\theta = 90^\circ$  as expected. Measurements at angles above  $80^\circ$  were not possible due to absorption and increasing background scattering from sample defects.

While the torque in a single-band superconductor is proportional to the misalignment,  $\delta\theta$ , this is not the case in materials with  $\gamma_\lambda \neq \gamma_H$  such as  $\text{MgB}_2$ . In the following it is assumed that the sample can be approximated by a oblate spheroid (a coin) with the  $c$  axis along  $z$ , and choosing  $(x, y)$  so that the applied field  $\mathcal{H}$  lies in the  $xz$ -plane forming an angle  $\theta$  with  $z$ . The linear relation between the applied field  $\mathcal{H}$ , the induction  $\mathbf{B}$ , and the magnetization  $\mathbf{M}$  reads:<sup>26</sup>

$$B_i = \mathcal{H}_i + 4\pi M_i(1 - n_i), \quad i = x, z, \quad (1)$$

where  $n_z = 1 - 2n$  and  $n_x = n$  are the demagnetization coefficients. For a coin-shaped sample  $n \ll 1$ . The angle,  $\theta_B = \theta - \delta\theta$ , between the induction and the  $c$  axis is given

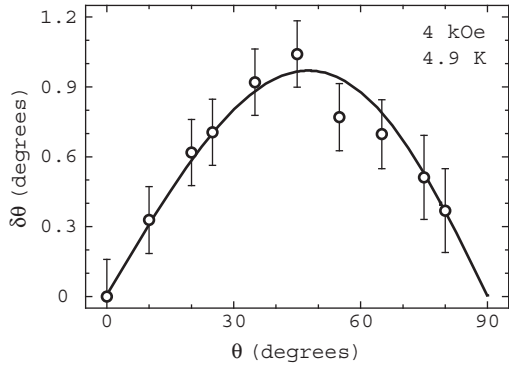


FIG. 3: FLL misalignment ( $\delta\theta$ ) as a function of the applied field rotation ( $\theta$ ). The error bars take into account both the statistical and systematic errors of the measurements. The solid line is a fit to the data described in the text.

by

$$\tan \theta_B = \frac{B_x}{B_z} = \frac{\mathcal{H}_x + 4\pi M_x(1 - n_x)}{\mathcal{H}_z + 4\pi M_z(1 - n_z)}. \quad (2)$$

For  $\mathcal{H} \gg H_{c1}$  where  $M \ll \mathcal{H}$ , as is the case in the present experiment, the misalignment  $\delta\theta = \theta - \theta_B$  is thus given

by:

$$\frac{\delta\theta}{2\pi} = \sin 2\theta \left[ \frac{M_z}{\mathcal{H}_z} 2n - \frac{M_x}{\mathcal{H}_x} (1 - n) \right]. \quad (3)$$

For materials with  $\gamma_\lambda \neq \gamma_H$  the free energy density is given by:<sup>6</sup>

$$\tilde{F} = F - \frac{B^2}{8\pi} = \frac{\phi_0 B \varepsilon_\lambda}{32\pi^2 \lambda^2 \gamma_\lambda^{1/3}} \ln \frac{4\eta H_{c2,c} \gamma_\lambda e}{B \varepsilon_\lambda (1 + \beta)^2}, \quad (4)$$

where  $\lambda = (\lambda_{ab}^2 \lambda_c)^{1/3}$  is the average penetration depth,  $\varepsilon_{\lambda,H}^2 = \sin^2 \theta_B + \gamma_{\lambda,H}^2 \cos^2 \theta_B$ , and

$$\beta = \frac{\gamma_\lambda}{\gamma_H} \sqrt{\frac{B_x^2 + \gamma_H^2 B_z^2}{B_x^2 + \gamma_\lambda^2 B_z^2}} = \frac{\gamma_\lambda \varepsilon_H}{\gamma_H \varepsilon_\lambda}. \quad (5)$$

The constant  $\eta$  lumps together the London uncertainty factor  $\approx 1.4$  with  $\pi\sqrt{3}/e$  yielding  $\eta \approx 2.8$ .

Evaluation of the magnetization,  $\mathbf{M} = -\partial\tilde{F}/\partial\mathbf{B}$ , and the misalignment angle,  $\delta\theta$ , is now straightforward. Differentiating with respect to  $(B_x, B_z)$ , and noting that  $B \varepsilon_\lambda = \sqrt{B_x^2 + \gamma_\lambda^2 B_z^2}$  one obtains  $\mathbf{M}$  in terms of  $\mathbf{B}$ :

$$\frac{M_x}{M_0} = -\frac{B_x \gamma_\lambda^{-1/3}}{B \varepsilon_\lambda} \left\{ \ln \frac{4\eta H_{c2,c} \gamma_\lambda}{(1 + \beta)^2 B \varepsilon_\lambda} + \frac{2\gamma_\lambda (\gamma_H^2 - \gamma_\lambda^2) \cos^2 \theta}{\gamma_H (1 + \beta) \varepsilon_\lambda \varepsilon_H} \right\}, \quad (6)$$

$$\frac{M_z}{M_0} = -\frac{B_z \gamma_\lambda^{5/3}}{B \varepsilon_\lambda} \left\{ \ln \frac{4\eta H_{c2,c} \gamma_\lambda}{(1 + \beta)^2 B \varepsilon_\lambda} - \frac{2(\gamma_H^2 - \gamma_\lambda^2) \sin^2 \theta}{\gamma_\lambda \gamma_H (1 + \beta) \varepsilon_\lambda \varepsilon_H} \right\}, \quad (7)$$

where  $M_0 = \phi_0/32\pi^2 \lambda^2$ . Since  $M \ll \mathcal{H}$ , the angle  $\delta\theta$  is small and  $M_i$ 's in Eq. (3) can be taken in the lowest

approximation. Substituting Eqs. (6) and (7) into Eq. (3) one can replace  $(B, \theta_B)$  with  $(\mathcal{H}, \theta)$  obtaining:

$$\frac{\delta\theta}{2\pi} = \frac{M_0 \sin 2\theta}{\mathcal{H} \gamma_\lambda^{1/3} \varepsilon_\lambda} \left\{ (1 - n - 2n\gamma_\lambda^2) \ln \frac{4\eta H_{c2,c} \gamma_\lambda}{(1 + \beta)^2 \mathcal{H} \varepsilon_\lambda} + \frac{2\gamma_\lambda (\gamma_H^2 - \gamma_\lambda^2)}{\gamma_H (1 + \beta) \varepsilon_\lambda \varepsilon_H} [(1 - n) \cos^2 \theta + 2n \sin^2 \theta] \right\}. \quad (8)$$

For MgB<sub>2</sub>,  $\gamma_H > \gamma_\lambda$  at all temperatures, and hence  $\delta\theta > 0$  for all values of  $\theta$  and  $T$  provided that  $n$  is small. Consequently, for a coin-shaped sample, the vortices are expected to rotate towards the *c* axis, consistent with the experimental results.

The solid line in fig. 3 is the best fit of Eq. (8) to the SANS data, obtained by varying  $\gamma_\lambda$  and  $\lambda$ , while setting  $\gamma_H = 6$ ,  $\eta = 2.8$  and using an approximate demagnetization factor for the sample,  $n = 0.01$ . This yields a value  $\gamma_\lambda = 1.1 \pm 0.2$  and  $\lambda = 155$  nm. This results pro-

vides additional evidence for a low value of  $\gamma_\lambda$  even at this relatively high field. Due to the uncertainty on the parameter  $\eta$  as well as the demagnetization factor,  $n$ , a reliable determination of  $\lambda$  and  $\gamma_H$  is difficult, especially since changing these two parameters both affects only the amplitude of  $\delta\theta$ . Nonetheless, the fitted value of  $\lambda$  is within the range of literature values summarized in Ref. [8] and in fair agreement with  $\lambda = 136$  nm from Ref. [16]. It should be noted that the profile of  $\delta\theta$  is determined solely by  $\gamma_\lambda$ , allowing a reliable fit of this pa-

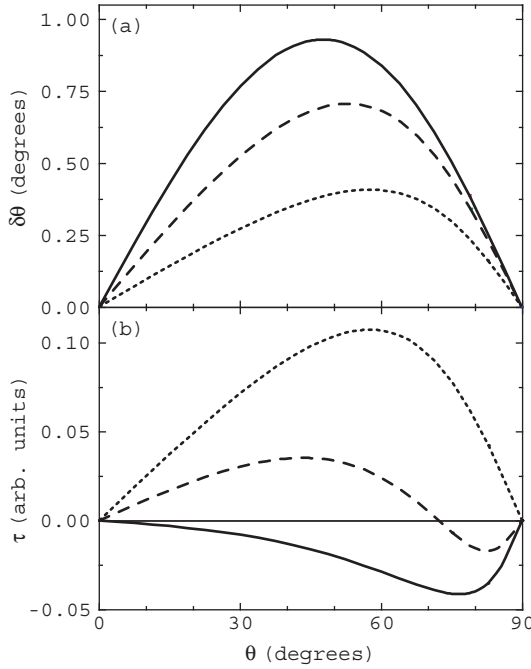


FIG. 4: Calculated misalignment (a) and torque (b) as a function of rotation angle, using Eqs. (8) and (9) with  $\mathcal{H} = 4$  kOe,  $\lambda = 155$  nm and  $n = 0.01$ . The curves corresponds to low ( $\gamma_H = 6, \gamma_\lambda = 1.1$ , solid line), intermediate ( $\gamma_H = 5.5, \gamma_\lambda = 1.5$ , dashed line) and high ( $\gamma_H = \gamma_\lambda = 2$ , dotted line) temperatures.<sup>7</sup>

parameter. Increasing  $\gamma_\lambda$  causes the  $\delta\theta$ -profile to become more asymmetric as shown in Fig. 4(a). Although it would be possible to fit our date with  $\gamma_H = \gamma_\lambda = 1.1$  and  $\lambda = 135$  nm, this is an unreasonably low value of  $\gamma_H$  for a field of 4 kOe, and consequently the results presented here do not support a single anisotropy factor as proposed in Refs. [14,16].

Before concluding, it is of interest to compare  $\delta\theta$  to the torque density,  $\tau_y = M_z \mathcal{H}_x - M_x \mathcal{H}_z$ . Inserting the  $M_i$ 's from Eqs. (6) and (7) one obtains:<sup>6</sup>

$$\tau_y = \frac{M_0 \mathcal{H} \sin 2\theta}{2\gamma_\lambda^{1/3} \varepsilon_\lambda} \left\{ (\gamma_\lambda^2 - 1) \ln \left( \frac{4\eta H_{c2,c} \gamma_\lambda}{(1 + \beta)^2 \mathcal{H} \varepsilon_\lambda} \right) - \frac{2\gamma_\lambda (\gamma_H^2 - \gamma_\lambda^2)}{\gamma_H (1 + \beta) \varepsilon_\lambda \varepsilon_H} \right\}. \quad (9)$$

Comparing this to Eq. (8) it is clear that in general  $\delta\theta$  is not proportional to  $\tau_y$  as only the former is shape dependent. In particular Eq. (9) suggests that at low temperature the torque is negative as shown in Fig. 4(b), in contrast to what has been observed for layered superconductors.<sup>27,28</sup> Near  $T_c$  one recovers  $\delta\theta \propto \tau_y$  as in materials with  $\gamma_\lambda = \gamma_H$ . Given the success of the model presented here in describing the misalignment, it would be of interest to test further the relationship between  $\delta\theta$  and the torque. Finally, one notes that for a spherical sample with  $n = 1/3$  one finds  $\delta\theta \propto \tau_y$  for all values of  $\gamma_\lambda$  and  $\gamma_H$ .

In summary we have shown that SANS measurements of the misalignment angle between the applied field and the FLL can provide information about the penetration

depth anisotropy in MgB<sub>2</sub>. At 4.9 K and 4 kOe we find a relatively low value of  $\gamma_\lambda = 1.1 \pm 0.2$ . More studies are needed to extend the measurements of  $\gamma_\lambda$  to both higher temperatures and fields, in order to investigate the entire mixed phase of MgB<sub>2</sub>.

#### Acknowledgments

We are grateful to J. Barker and P. Butler for their help during the SANS experiment. We acknowledge the support of the National Institute of Standards and Technology, U.S. Department of Commerce, in providing the neutron research facilities used in this work. This work utilized facilities supported in part by the National Science Foundation under Agreement No. DMR-0454672.

\* Electronic address: eskildsen@nd.edu

<sup>1</sup> A comprehensive review can be found in Physica C **385** (1-

2) (2003), special issue, edited by W. Kwok, G. Crabtree, S. L. Bud'ko, and P. C. Canfield.

<sup>2</sup> J. Kortus, I. I. Mazin, K. D. Belashchenko, V. P. Antropov, and L. L. Boyer, Phys. Rev. Lett. **86**, 4656 (2001).

<sup>3</sup> A. Y. Liu, I. I. Mazin, and J. Kortus, Phys. Rev. Lett. **87**, 087005 (2001).

<sup>4</sup> H. J. Choi, D. Roundy, H. Sun, M. L. Cohen and S. G. Louie, Nature (London), **418**, 758 (2002).

<sup>5</sup> V. G. Kogan, Phys. Rev. B **66** 020509(R) (2002).

<sup>6</sup> V. G. Kogan, Phys. Rev. Lett. **89**, 237005 (2002).

<sup>7</sup> P. Miranović, K. Machida, and V. G. Kogan, J. Phys. Soc. Japan **72**, 221 (2003).

<sup>8</sup> A. A. Golubov, A. Brinkman, O. V. Dolgov, J. Kortus and O. Jepsen, Phys. Rev. B **66** 054524 (2002).

<sup>9</sup> F. Simon *et al.*, Phys. Rev. Lett. **87** 047002 (2001).

<sup>10</sup> G. Papavassiliou, M. Pissas, M. Fardis, M. Karayanni and C. Christides, Phys. Rev. B **65**, 012510 (2001).

<sup>11</sup> M. Angst *et al.*, Phys. Rev. Lett. **88**, 167004 (2002).

<sup>12</sup> S. L. Bud'ko and P. C. Canfield, Phys. Rev. B **65**, 212501 (2002).

<sup>13</sup> M. Zehetmayer *et al.*, Phys. Rev. B **66**, 052505 (2002).

<sup>14</sup> L. Lyard *et al.*, Phys. Rev. Lett. **92**, 057001 (2004).

<sup>15</sup> A. Rydh *et al.*, Phys. Rev. B **70**, 132503 (2004)

<sup>16</sup> M. Angst *et al.*, Phys. Rev. B **70**, 224513 (2004).

<sup>17</sup> R. Cubitt, S. Levett, S. L. Bud'ko, N. E. Anderson, and P. C. Canfield, Phys. Rev. Lett. **90**, 157002 (2003).

<sup>18</sup> M. R. Eskildsen *et al.*, Phys. Rev. B **68**, 100508(R) (2003).

<sup>19</sup> J. D. Fletcher, A. Carrington, O. J. Taylor, S. M. Kazakov, and J. Karpinski Phys. Rev. Lett. **95**, 097005 (2005).

<sup>20</sup> R. Cubitt *et al.*, Phys. Rev. Lett. **91**, 047002 (2003).

<sup>21</sup> F. Bouquet *et al.*, Phys. Rev. Lett. **89**, 257001 (2002).

<sup>22</sup> J. Karpinski *et al.*, Supercond. Sci. Technol. **16**, 221 (2003).

<sup>23</sup> M. E. Zhitomirsky and V.-H. Dao, Phys. Rev. B **69**, 054508 (2004).

<sup>24</sup> R. Cubitt, M. R. Eskildsen and C. D. Dewhurst, to be published.

<sup>25</sup> M. R. Eskildsen *et al.*, Phys. Rev. Lett. **86**, 320 (2001).

<sup>26</sup> L. D. Landau, E. M. Lifshitz, and L. P. Pitaevskii, *Electrodynamics of Continuous Media*, 2nd ed. (Pergamon Press, Oxford, 1984), §29.

<sup>27</sup> J. M. Tranquada *et al.*, Phys. Rev. B **37**, 519 (1988).

<sup>28</sup> D. E. Farrell, C. M. Williams, S. A. Wolf, N. P. Bansal, and V. G. Kogan, Phys. Rev. Lett. **61**, 2805 (1988)